Stem Cell Reports
Article

OPEN ACCESS

Polycomb Protein EED Regulates Neuronal Differentiation through Targeting SOX11 in Hippocampal Dentate Gyrus

Pei-Pei Liu,[1,4,5] Ya-Jie Xu,[1,2,4,5] Shang-Kun Dai,[1,2,4] Hong-Zhen Du,[1,4] Ying-Ying Wang,[1,2,4] Xing-Guo Li,[3] Zhao-Qian Teng,[1,2,4] and Chang-Mei Liu[1,2,4,*]

[1]State Key Laboratory of Stem Cell and Reproductive Biology, Institute of Zoology, Chinese Academy of Sciences, Beijing, China
[2]Savaid Medical School, University of Chinese Academy of Sciences, Beijing 100049, China
[3]Department of Pediatrics, James P. Wilmot Cancer Center, University of Rochester Medical Center, Rochester, NY 14642, USA
[4]Institute for Stem Cell and Regeneration, Chinese Academy of Sciences, Beijing 100101, China
[5]Co-first author
*Correspondence: liuchm@ioz.ac.cn
https://doi.org/10.1016/j.stemcr.2019.05.010

SUMMARY

EED (embryonic ectoderm development) is a core component of the Polycomb repressive complex 2 (PRC2) which catalyzes the methylation of histone H3 lysine 27 (H3K27) during the process of self-renewal, proliferation, and differentiation of embryonic stem cells. However, its function in the mammalian nervous system remains unexplored. Here, we report that loss of EED in the brain leads to postnatal lethality, impaired neuronal differentiation, and malformation of the dentate gyrus. Overexpression of *Sox11*, a downstream target of EED through interaction with H3K27me1, restores the neuronal differentiation capacity of EED-ablated neural stem/progenitor cells (NSPCs). Interestingly, downregulation of *Cdkn2a*, another downstream target of EED which is regulated in an H3K27me3-dependent manner, reverses the proliferation defect of EED-ablated NSPCs. Taken together, these findings established a critical role of EED in the development of hippocampal dentate gyrus, which might shed new light on the molecular mechanism of intellectual disability in patients with EED mutations.

INTRODUCTION

Polycomb group (PcG) proteins are highly conserved transcriptional repressors that epigenetically modify chromatin and participate in the establishment or maintenance of cell fates (Hirabayashi et al., 2009). Mounting evidence has shown that PcG proteins are involved in regulating many dynamic processes such as cellular proliferation, senescence, and differentiation of functional neural cell types (Pereira et al., 2010; von Schimmelmann et al., 2016). There are mainly two functionally distinct polycomb repressive complexes (PRCs), PRC1 and PRC2. PRC2 typically contains the core components SUZ12, embryonic ectoderm development (EED), and enhancer of zeste homolog 2 (EZH2), to constitute the histone methyltransferase complex responsible for catalyzing histone H3 lysine 27 trimethylation (H3K27me3). PRC2 complexes are essential for the maintenance of neural stem/progenitor cells (NSPCs) and the generation of functional neural cell types. For example, conditional deletion of the PRC2 component EZH2 in the early developing forebrain results in a shortened period of neuronal production due to a lack of precursor cell proliferation and premature NSPC differentiation (Pereira et al., 2010). Although several components of PRC2 have been investigated in brain development or neurogenesis, very little is known about the role and the mechanism of action of EED.

EED is required for EZH2 and SUZ12 stability, and it mediates the epigenetic repressive H3K27me3 mark through a positive feedback loop by binding to H3K27me3 and subsequently activating the methyltransferase activity of EZH2 (Margueron et al., 2009). A very early report from EED-deficient mice suggested that EED might be a key regulator of neurogenesis (Schumacher et al., 1996). Clinical data showed that EED mutations are related to Weaver syndrome, an autosomal dominant disease characterized by learning disabilities, dysmorphic facial features, and general overgrowth (Cooney et al., 2017). Mechanistically, increasing evidence has demonstrated that learning and memory disorders are usually linked to abnormal neurogenesis and dentate gyrus (DG) formation (Imagawa et al., 2017; Zhang et al., 2014), which provides strong support for the idea that EED might be an important regulator of intelligence-associated brain development. Therefore, we hypothesized that mutations in EED may result in abnormal hippocampal neurogenesis or DG malformation.

To test our hypothesis, we used a conditional knockout "floxed" allele of *Eed* ($Eed^{f/f}$) to investigate the role of EED in hippocampal development. By crossing $Eed^{f/f}$ mice with the transgenic mouse hGFAP-*Cre* (Zhuo et al., 2001), EED was specifically deleted in NSPCs from embryonic day 13.5 (E13.5).

Disruption of EED resulted in postnatal lethality, impaired migration of granule cells, loss of the subgranular zone (SGZ), and severely disrupted secondary radial glial scaffold in the hippocampus. Mechanistically, overexpression of *Sox11*, a downstream target of EED, restored the neuronal differentiation ability of EED-ablated NSPCs.

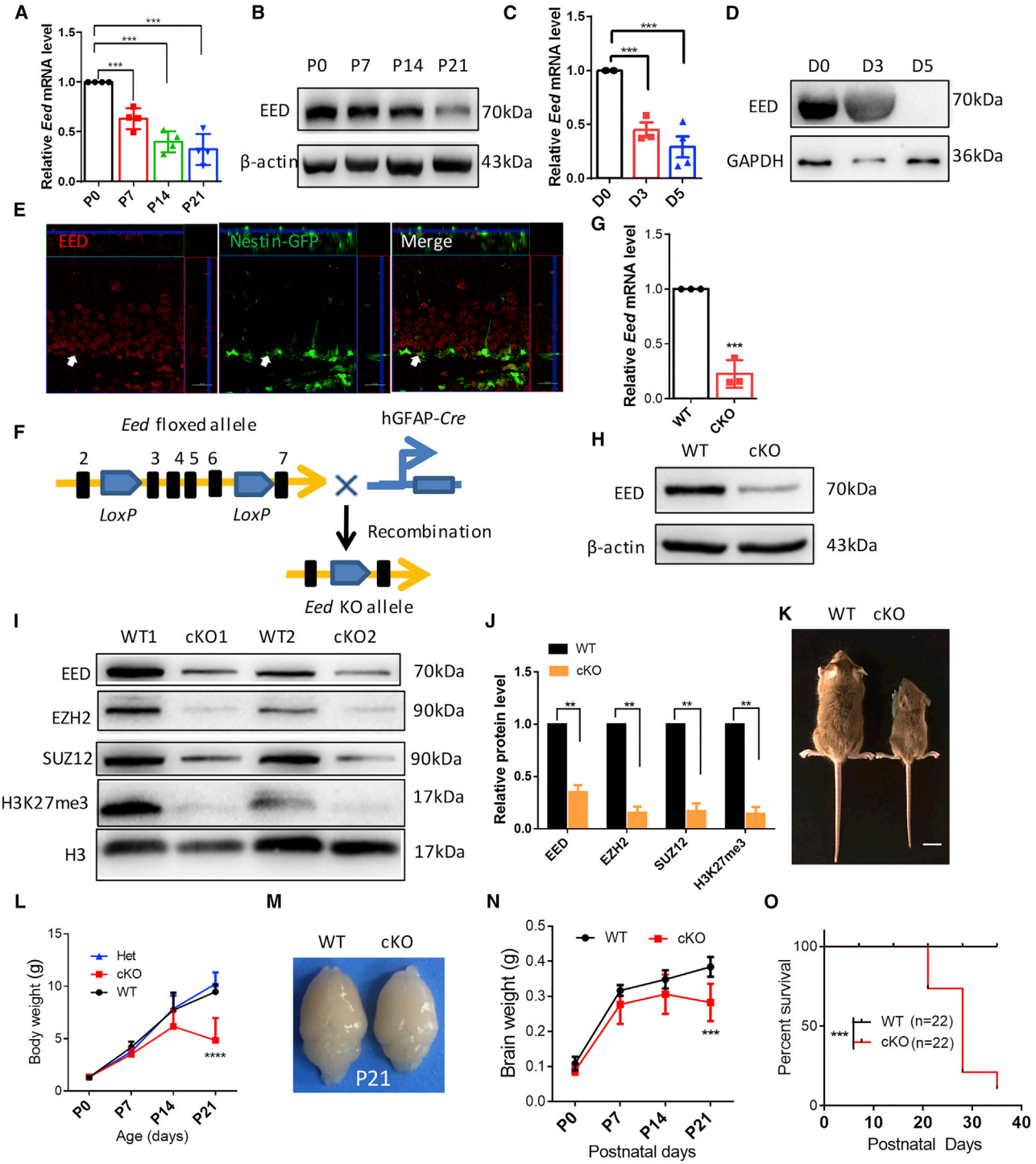

Figure 1. EED Is Highly Expressed in the Developing Hippocampus and Deletion of EED Leads to Postnatal Lethality and Reduced Brain Weight

(A and B) Expression levels of EED in mice hippocampus tissues during development from postnatal day 0 to 21. *Eed* mRNA level was measured by qPCR (A) (n = 4 mice) and protein level was quantified by western blot with the antibodies indicated on the left in (B), β-actin was used as loading controls. For P7, ***p = 0.0004; for P14, ****p < 0.0001; for P21, ***p = 0.0001.

(C and D) EED expression level in dissociated neural stem cells/progenitor cells (NSPCs) isolated from the DG of P0 mice in proliferation conditions (day 0) or in differentiation conditions (days 3 and 5). *Eed* mRNA expression level was quantified using real-time qPCR in

(legend continued on next page)

On the other hand, directly repressing *Cdnk2a*, another downstream target of EED in NSPCs, reversed the proliferation defect of EED-deleted NSPCs. These results highlight the critical role of EED in a series of essential events that cumulatively orchestrate the developmental formation of the DG, and thus provide molecular evidence supporting that dysregulation of EED may contribute to the cause of Weaver syndrome.

RESULTS

EED Is Highly Expressed in NSPCs and Conditional EED Deletion in the CNS Results in Postnatal Lethality

To explore the developmental dynamics of EED in the mammalian brain, we examined its expression at both mRNA and protein levels. *Eed* was expressed robustly at postnatal day 0 (P0), and the expression level declined but continued to occur afterward in the microdissected cortex and hippocampus tissues for both mRNA (Figures S1A and 1A) and protein levels (Figures S1B and 1B). Real-time qPCR and western blot results suggest that the expression level of *Eed* was higher in NSPCs than that in differentiated progenies (Figures S1C, S1D, 1C, and 1D), which indicates the possible involvement of EED in maintaining neural stem cells (NSCs) at postnatal periods.

To confirm the expression of EED in NSPCs, we analyzed immunohistochemical EED expression in brain tissues of 1-month-old Nestin-GFP mice and found that EED was indeed present in the GFP^+ cells (Figure 1E). We then assessed the EED expression pattern in the DG by co-immunostaining EED with a variety of cell fate markers. EED was broadly expressed in the DG, especially in nearly all $NeuN^+$ mature neuron cells, $GFAP^+$ cells (which include quiescent NSCs and astrocytes), and $Olig2^+$ (a mark of oligodendrocyte) cells (Figure S1E). These results suggest that EED may function throughout the entire course of neurogenesis.

To delete EED from NSPCs and their progeny, we created $Eed^{f/f}$;hGFAP-Cre^+ (hereafter referred to as cKO) by crossing $Eed^{f/f}$ with hGFAP-*Cre* transgene mice (Figure 1F), which drives *Cre*-mediated recombination in the precursors of the cerebellar granule cell layer, hippocampal DG, and the subventricular zone (SVZ) (Han et al., 2008). In the presence of *Cre* recombinase, exons 3–6 of *Eed* flanked by *loxP* sites were deleted, resulting in a frameshift that leads to minimal RNA and protein expression (Figures 1G and 1H). Immunoblot analysis confirmed the absence of EED protein, as well as a significant reduction in EZH2, SUZ12, and global H3K27me3 levels in EED cKO P14 hippocampus (Figures 1I and 1J). EED cKO mice were born at the expected Mendelian ratios, showed no overt developmental or morphologic abnormalities between P0 and P7 (Figure S1F). However, by P14, EED cKO mice developed progressive growth retardation and ataxia, as these animals had significantly reduced body weight and brain weight than wild-type (WT) mice (Figures 1K–1N). As EED cKO mice usually died between P21 and P30 (Figure 1O), we therefore analyzed these animals at P14–P21.

Lack of EED Leads to Developmental Malformation of the Postnatal DG

As EED has been implicated as a critical regulator for the maintenance of stem cells, including NSPCs (Satijn et al., 2001; Shen et al., 2008; Xie et al., 2014), we first performed histological studies in the DG and SVZ, where postnatal NSPCs reside. We observed a thinner SVZ in EED cKO mice at P21 compared with WT littermates (Figures S2A

(C) (n = 3 at least) and protein level was quantified with western blot with the EED antibody indicated at left in (D), GAPDH were used as loading controls. For D3, ***p = 0.0002; for D5, ***p = 0.0003.
(E) Immunofluorescence of 1-month-old Nestin-GFP mice, EED (red) colocalized with the progenitor marker Nestin (green) within the dentate gyrus.
(F) Schematic diagram for the generation of GFAP-*Cre*-mediated EED knockout mice. Exons 3–6 of the *Eed* allele are flanked by *loxP* sites and depleted in the presence of *Cre* recombinase, resulting in null alleles.
(G and H) Expression level of *Eed* in WT and EED cKO mice was shown by real-time qPCR (G) (n = 3 mice) and western blot (H) using P14 DG tissues. ***p = 0.0004.
(I) Expression levels of the indicated PRC2 components (EED, EZH2, and SUZ12) and H3K27me3 methylation were quantified by western blot analysis of P14 DG protein lysates in EED cKO mice (n = 3). Histone H3 is used as the loading control. A representative image is shown.
(J) Quantification of the western blot in (I). Histone H3 bands were used for normalization. **p < 0.01.
(K) EED cKO become runted by P21 compared with littermate controls. Scale bar, 100 μm.
(L) EED cKO mice had reduced body weight at P21 compared with the control littermates (n = 4 mice per genotype at least). For P21, ****p < 0.0001.
(M) Dorsal view of WT and EED cKO by P21 brains.
(N) EED cKO mice had reduced brain weight at P21 compared with the control littermate (n = 3 mice per genotype at least). For P21, ***p = 0.0003.
(O) Kaplan-Meier survival curve of WT and cKO mice over a 40-day period (n = 22 WT and 22 cKO). ***p < 0.001.

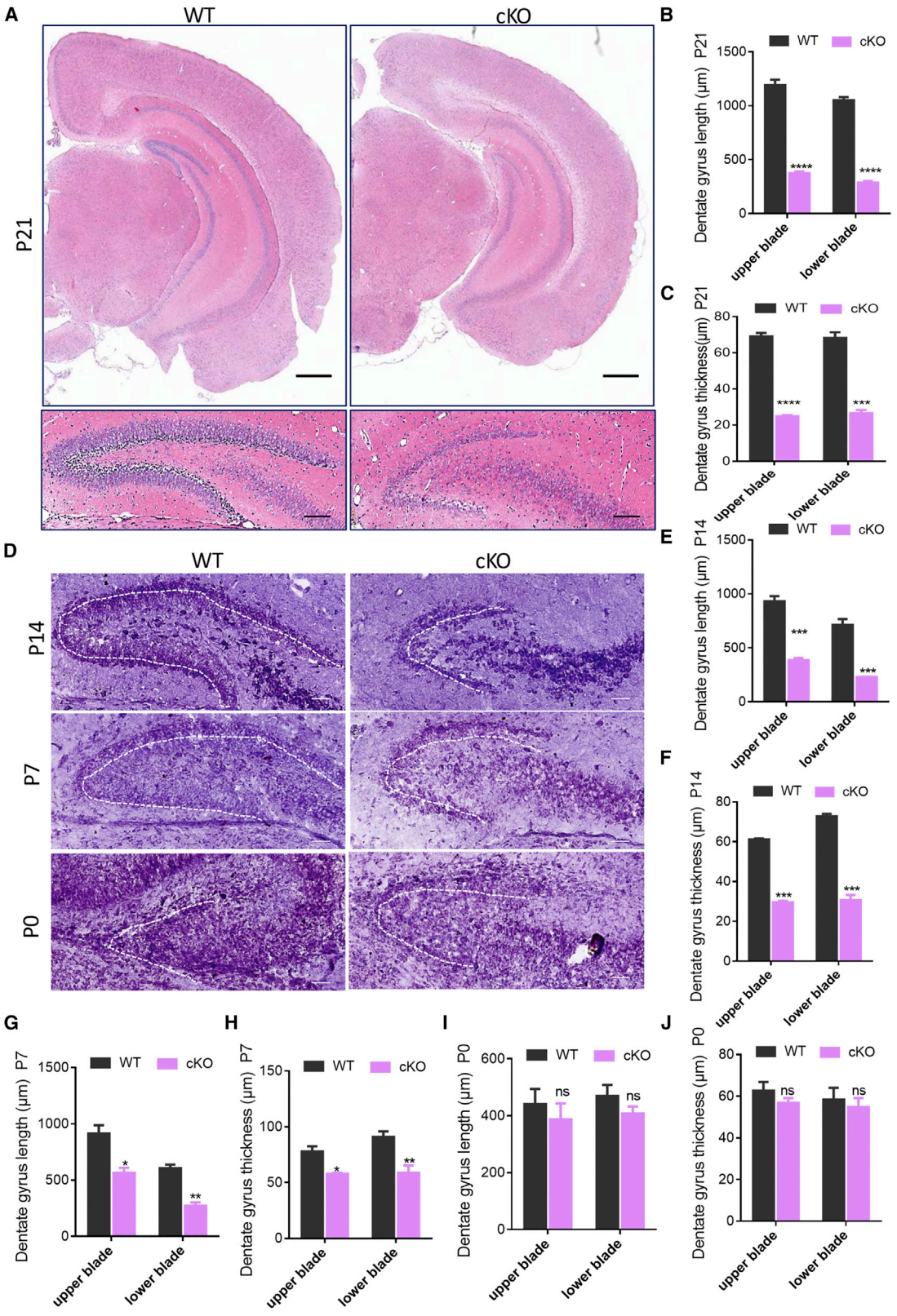

(legend on next page)

and S2B). Similarly, histological analysis of mutant mice revealed striking abnormalities in hippocampal formation (Figures 2A, S2C, and S2D). These results suggest a common requirement for EED in neurogenesis. Notably, the gross structures of hippocampus were normal, as indicated by immunostaining for the neuronal marker NeuN (Figure S2C). Under higher magnification, the pyramidal cell layer of the hippocampal CA1 and CA3 regions also showed apparently normal morphology and cellular organization in the EED cKO mice when compared with WT mice (Figures S2E–S2H). However, severe abnormalities were observed in the DG of EED cKO mice (Figures 2A and S2C), suggesting that EED might be an important modulator for hippocampal DG neurogenesis and formation. We therefore focused our efforts on the hippocampal DG development where NSPCs reside and differentiate into a rudimentary population of neurons. To analyze the developmental stage at which these phenotypes first emerge, coronal sections from P0 to P14 hippocampal DG were examined. Cresyl violet (Nissl) staining of EED cKO brains at P0 showed apparently normal morphology and cellular organization in the DG (Figures 2D, 2I, and 2J). Importantly, clear hippocampal retardation became evident at P7 (Figures 2D, 2G, and 2H), a critical stage for DG development. Quantification of the length and thickness of the blades of the DG revealed that both the upper and lower blades of EED cKO DGs were shorter in comparison with the WT control (Figures 2D, 2G, and 2H). By P14, we also observed a significant decrease in the DG area of EED cKO mice (Figures 2D–2F), suggesting a possible failure of NSPC-driven neurogenesis in EED cKO mice. Taken together, these experiments demonstrate that EED plays a critical role in hippocampal DG development.

EED Deletion Leads to Dynamic Changes of DG Cell Compartments

As the scaffolding of the DG forms at approximately the first postnatal week, precursors migrate into the DG and settle in the SGZ at the border between the granular layer and the hilus. The SGZ thus provides a steady flow of newborn cells at postnatal stages (Steiner et al., 2004). We reason that the remarkably reduced size of DGs in EED cKO mice may be accompanied by a dynamic change in DG cell (DGC) compartments. To test this notion, we first assessed the role of EED in postnatal NSPCs in the DG and in the development of the radial glial scaffold by immunostaining GFAP to label both NSPCs and astrocytes. We found that deletion of EED significantly reduced $GFAP^+$ cells compared with WT mice at P7 (Figures 3A and 3B). Similarly, the relative number of $GFAP^+$ cells was also decreased in EED cKO DGs relative to WT at both P14 and P21 (Figures 3C–3F). These data suggest that the EED activity contributes to the organization of astrocytic fate.

Next, to determine whether neurons are affected following EED ablation, we labeled mature neurons by immunostaining for NeuN. The number of postmitotic neurons was transiently increased in P7 EED cKO DGs, but then decreased dramatically at P14 and P21 in contrast to WT DGs (Figure 3G). Then, to assess the role of EED in dentate granule neuron formation, we analyzed the expression of dentate-specific *Prox1* in WT and EED cKO mice. In WT hippocampus, PROX1-expressing dentate granule neurons were present within the DG at P7, P14, and P21, and these cells were localized within the blades of the DG (Figure 3H). In the EED cKO mice, however, there were fewer PROX1-expressing cells within the hippocampus per unit length (Figures 3H and 3I). Consistent with previous reports (Freund and Buzsaki, 1996), interneurons throughout the hippocampus of young and mature animals were positive for calbindin. Furthermore, the production of $calbindin^+$ interneurons and their subsequent migration into the hippocampus occurred abnormally from P7 onward until P21 in EED cKO mice (Figures 3J and 3K). Taken together, these data suggest that although the morphogenesis of the DG does eventually occur in EED cKO mice, fewer dentate

Figure 2. Lack of EED Leads to Developmental Malformation of the Postnatal DG

(A) Top, H&E staining of cerebrum coronal sections from WT and EED cKO mice at P21. Scale bars, 500 μm. Bottom, higher magnification of dentate gyrus of hippocampus is shown in the panels. Note the presence of abnormal DG in EED cKO mice. Scale bars, 100 μm.

(B and C) The measurement of the lengths (B) and the thickness (C) of the dentate gyrus blades revealed that both the upper and lower blades of the EED cKO were significantly shorter than those of their WT littermate controls at P21 (n = 3 repeats at least). ***p < 0.001, ****p < 0.0001.

(D) Cresyl violet staining of P14, P7, and P0 hippocampus sections. Brains were isolated from mice after transcranial perfusion with 4% paraformaldehyde. Coronal sections of the cerebrum were subjected to Cresyl violet staining. The horizontal check mark-shaped dense granule cell zones defined by dotted lines are the DG. Left to right, anterior to posterior. Scale bars, 100 μm.

(E–H) The measurement of the lengths (E and G) and the thickness (F and H) of the dentate gyrus blades revealed that both the upper and lower blades of the EED cKO were significantly shorter than those of their WT littermate controls at P14 and P7 (n = 3 repeats at least). *p < 0.05, **p < 0.01, ***p < 0.001.

(I and J) Similar lengths (I) and thickness (J) of the blades of the dentate gyrus at P0 in WT and EED cKO mice (n = 3 repeats at least). ns, nonsignificant.

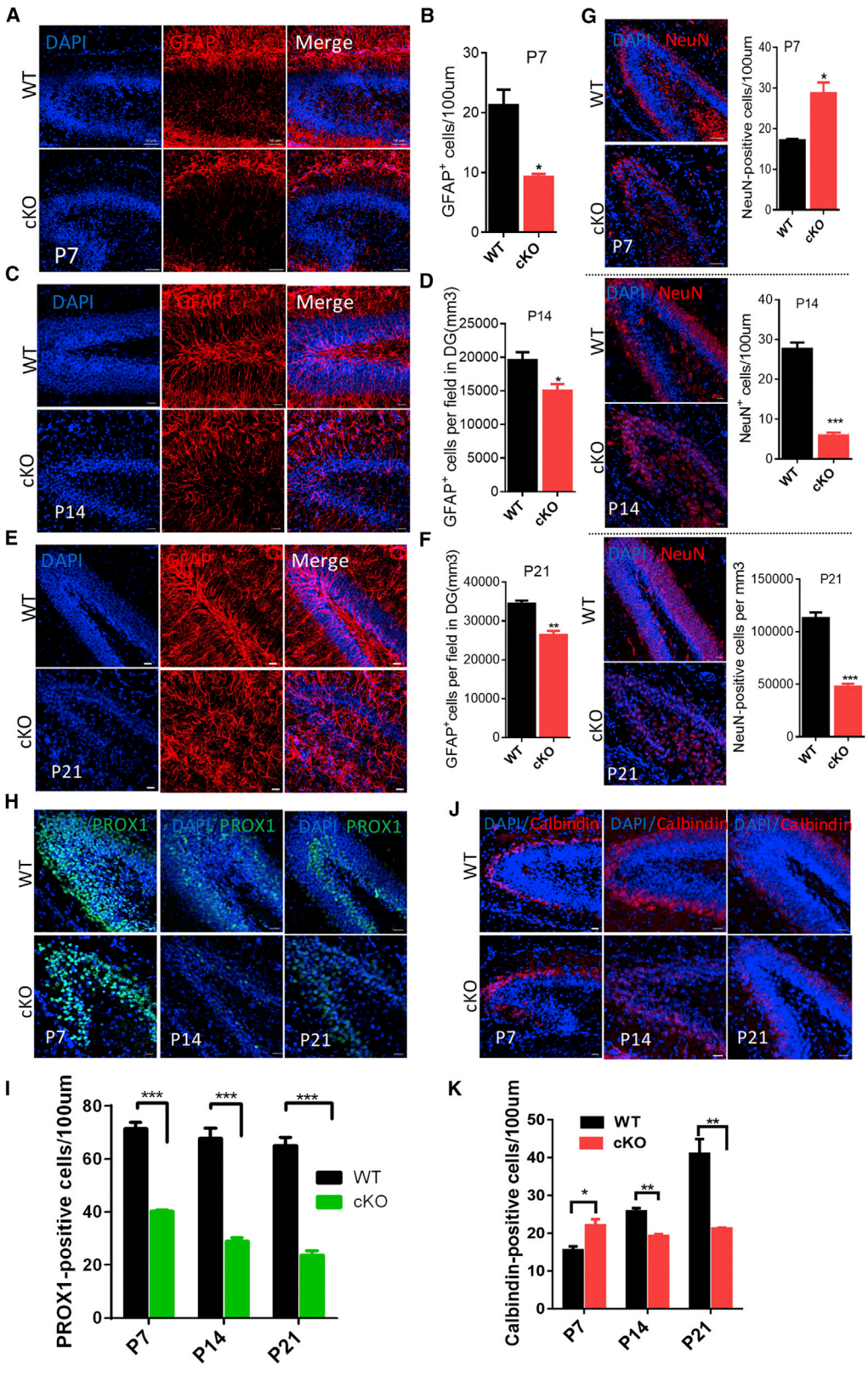

(legend on next page)

granule neurons ultimately populate postnatal DG in these animals.

We then asked whether EED ablation affects oligodendrocyte cells by performing Olig2 immunostaining on EED cKO and WT mice. At P7, compared with WT mice, there were >1.6-fold more Olig2$^+$ cells in the DG of EED cKO mice (Figures S3A and S3D). Our analysis of Olig2$^+$ cells in P14 mice showed that there were also more Olig2$^+$ cells within the hippocampal SGZ of EED cKO mice than those within WT mice (Figures S3B and S3D). However, at P21, there was no difference in the number of Olig2$^+$ cells between EED cKO and WT mice (Figures S3C and S3D). These findings suggest that loss of EED biases postnatal NSPCs toward oligodendrogenesis at the early postnatal stage.

EED Ablation Results in Aberrant Neuronal Differentiation during Postnatal DG Development

To accurately monitor the neuronal differentiation ability, mice were administered 5-bromo-2-deoxyuridine (BrdU) at P10 and brains were harvested at P17 to detect the long-term effect of EED deletion on hippocampus neurogenesis. We found a marked reduction in the number of NeuN and BrdU double-labeled cells in the EED cKO mice (Figures 4A and 4B), indicating that loss of EED had a long-term effect on neuronal differentiation. We next examined the differentiation ability of NSPCs *in vitro* by plating the same number of NSPCs from P0 EED cKO and WT DG in the differentiation medium. We observed fewer neurons formed (Tuj1$^+$) from EED cKO NSPCs than those from WT NSPCs (Figures 4C and 4D). Therefore, these results suggest that the EED cKO DG has a striking defect in neuronal differentiation ability both *in vivo* and *in vitro*.

In the postnatal and adult periods, immature DGCs are continuously generated from proliferating progenitor cells located in the SGZ. These cells migrate only a short distance into the granule cell layer and then terminally differentiate into new DGCs. We therefore asked whether the migration of mitotic precursor cells to the DG is abnormal in mutant mice. To test this idea, we firstly examined cells expressing doublecortin (DCX), a microtubule-associated protein required for neuronal migration and used as a marker of immature neurons at P21. Quantitative analyses demonstrated that EED cKO mice had much lower density of DCX$^+$ immature DGCs (Figures 4E and 4F). The number of DCX$^+$ cells was also sharply decreased at P14 in EED cKO mice (Figures 4G and 4H), indicating that depletion of EED led to fewer neuronal cells in DG.

EED Is Required for NSPCs Self-Renewal in the DG

To explore the potential role of EED in modulating NSPC properties, we examined the number of NSPCs in the DG and their progeny by using various lineage markers. In the P7 brain sections, the number of dividing cells (Ki67$^+$ cells) in the DG region was reduced significantly in EED cKO mice (Figures 5A and 5B). We further examined the rate of BrdU incorporation into P14 and P21 DGCs. Compared with WT mice, EED cKO mice showed dramatic reductions of BrdU incorporation and Ki67$^+$ cells at both ages (Figures 5C–5F), indicating that deletion of EED impaired the proliferation of NSPCs in the DG.

To further confirm the role of EED in postnatal NSPC proliferation and self-renewal, we compared isolated NSPCs using a neurosphere assay. NSPCs from P0 DG of WT and EED cKO mice gave rise to primary neurospheres starting from day 4 of culture in the aerosphere medium. At day 7, we measured the diameter of primary neurospheres as an indicator of the size of NSPCs and the neurospheres were then passaged every week. We found that EED cKO NSPCs formed much fewer and smaller primary neurospheres compared with those from WT mice (Figures 5G and 5H), indicating that there were fewer self-renewing NSPCs in the EED cKO DG. Furthermore, the neurosphere-forming NSPCs isolated from EED cKO DG did not further divide and displayed significantly lower viability compared with WT NSPCs (Figures 5G and 5H), indicating

Figure 3. Dynamic Changes of Cell Compartments in the DG following EED Deletion

(A) Immunofluorescence for GFAP (red) in the DG from WT and EED cKO mice at P7.

(B) Quantification of GFAP$^+$ cell numbers in (A) (n = 3 mice). Scale bars, 50 μm. *p = 0.0108.

(C–F) Representative images of GFAP immunostaining in the DG from WT and EED cKO mice at P14 and P21 (C and E). An abnormal decrease in GFAP$^+$ cells was detected in EED cKO DG (D and F) (n = 3 mice). Scale bars, 20 μm. For P14, *p = 0.0427; for P21, **p = 0.0036.

(G) Left, representative sections of the DG stained with the mature neuron marker NeuN (red) at P7, P14, and P21 (n = 3 mice). Right, quantification of the NeuN$^+$ cells in the DG following EED deletion at P7, P14, and P21. Scale bars, 20 μm. For P7, *p = 0.0120; for P14, ***p = 0.0002; for P21, ***p = 0.0004.

(H) Representative images of the dentate granule cell marker PROX1 (green) staining in the DG of WT and EED cKO mice at P7, P14, and P21.

(I) Quantification of Prox1-expressing cells revealed significantly fewer dentate granule cells within the DG of EED cKO mice at P7, P14, and P21 (n = 3 mice). Scale bars, 20 μm. For P7, ***p = 0.0002; for P14, ***p = 0.0006; for P21, ***p < 0.001.

(J) Representative images of calbindin (red) staining in coronal sections of WT and EED cKO mice at P7, P14, and P21.

(K) Quantification of calbindin-expressing cells within the DG of WT and EED cKO mice at P7, P14, and P21 (n = 3 mice). Scale bar, 20 μm. For P7, *p = 0.0242; for P14, **p = 0.0031; for P21, **p = 0.0073.

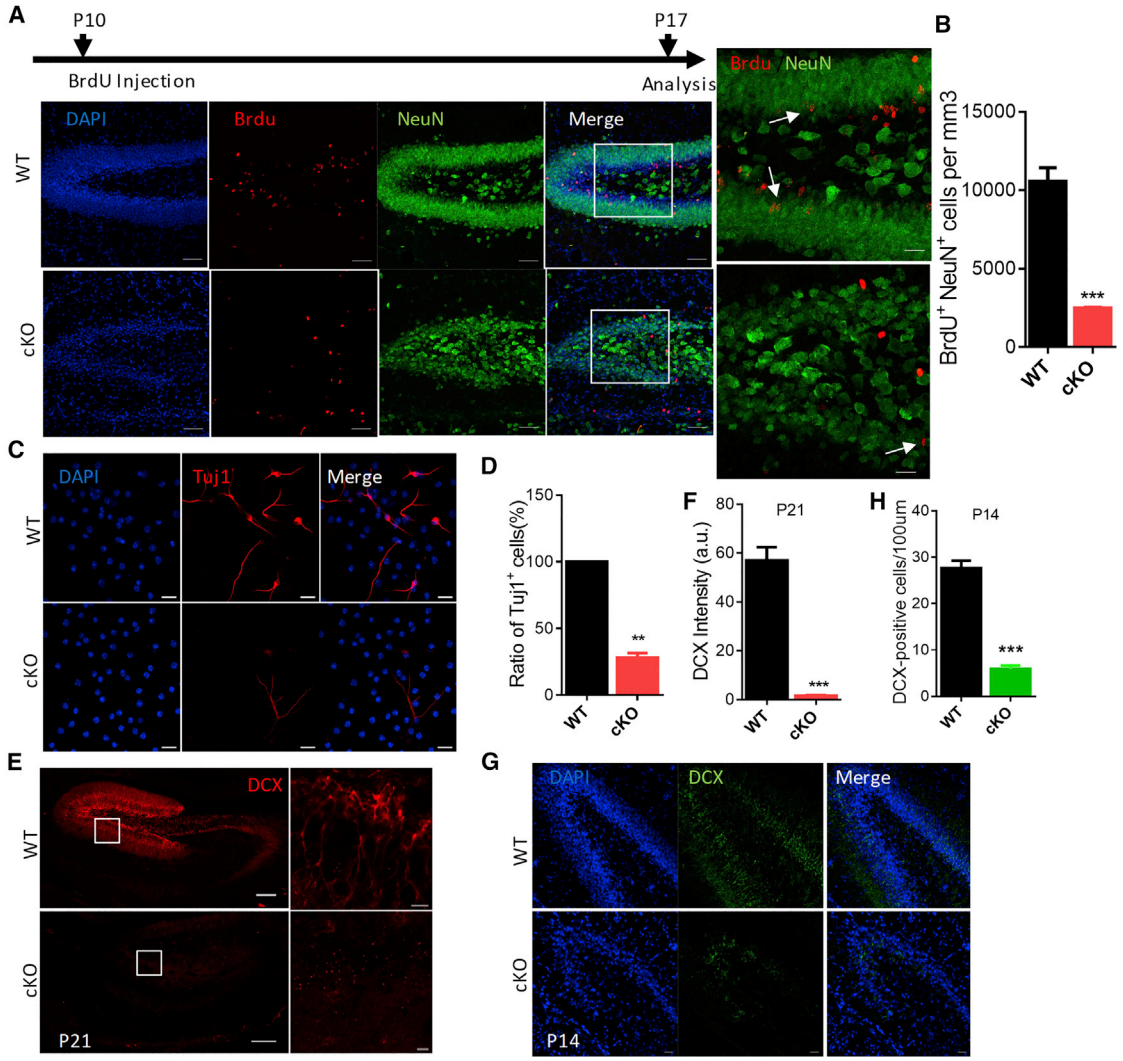

Figure 4. Deletion of EED in DG NSPCs Inhibits Neurogenesis Both *In Vivo* and *In Vitro*

(A) Representative sections of the DG stained with the mature neuron marker NeuN (green) and the proliferation marker BrdU (red) from WT and EED cKO mice at P17. Mice at P10 were injected intraperitoneally with BrdU to detect newborn neurons *in vivo* and monitored for 7 days. Scale bars, 50 μm. The regions within the white boxes are shown at a higher magnification in adjacent panels. Scale bars, 20 μm. Arrowheads indicate BrdU and NeuN double-positive cells.

(B) Quantitative analysis of the reduced number of new neurons (BrdU and NeuN double-labeled cells) observed in (A) (n = 3 mice). ***p = 0.0007.

(C) Immunostaining for neuronal marker Tuj1 (red) after 10 days of differentiation in cultured WT and EED cKO NSPCs.

(D) Quantification of Tuj1$^+$ cells as a percentage of total cells after 10 days of differentiation in cultured WT and EED cKO NSPCs (n = 5 WT and 3 cKO), Scale bars, 20 μm. **p < 0.01.

(E) Representative doublecortin (DCX) (red) staining on coronal DG sections from WT and EED cKO mice at P21. Scale bars, 100 μm. The regions of the hilus within white boxes in the upper panels are shown at a higher magnification in adjacent panels. Scale bars, 10 μm.

(F) Comparison of DCX intensity of WT and EED cKO mice at P21. All pictures were taken with the same exposure time to evaluate DCX intensity using ImageJ (n = 3 mice). ***p = 0.0005.

(G) DG sections of WT and EED cKO mice at P14 were stained with DCX (green) antibody. Scale bars, 20 μm.

(H) Quantification of the number of DCX$^+$ cells in the DG of WT and EED cKO mice at P14 (n = 3 mice). Data are expressed as the means ± SE, and comparisons between WT and EED cKO mice were done by Student's t test (n = 3 mice). Scale bars, 20 μm. ns, nonsignificant. ***p = 0.0002.

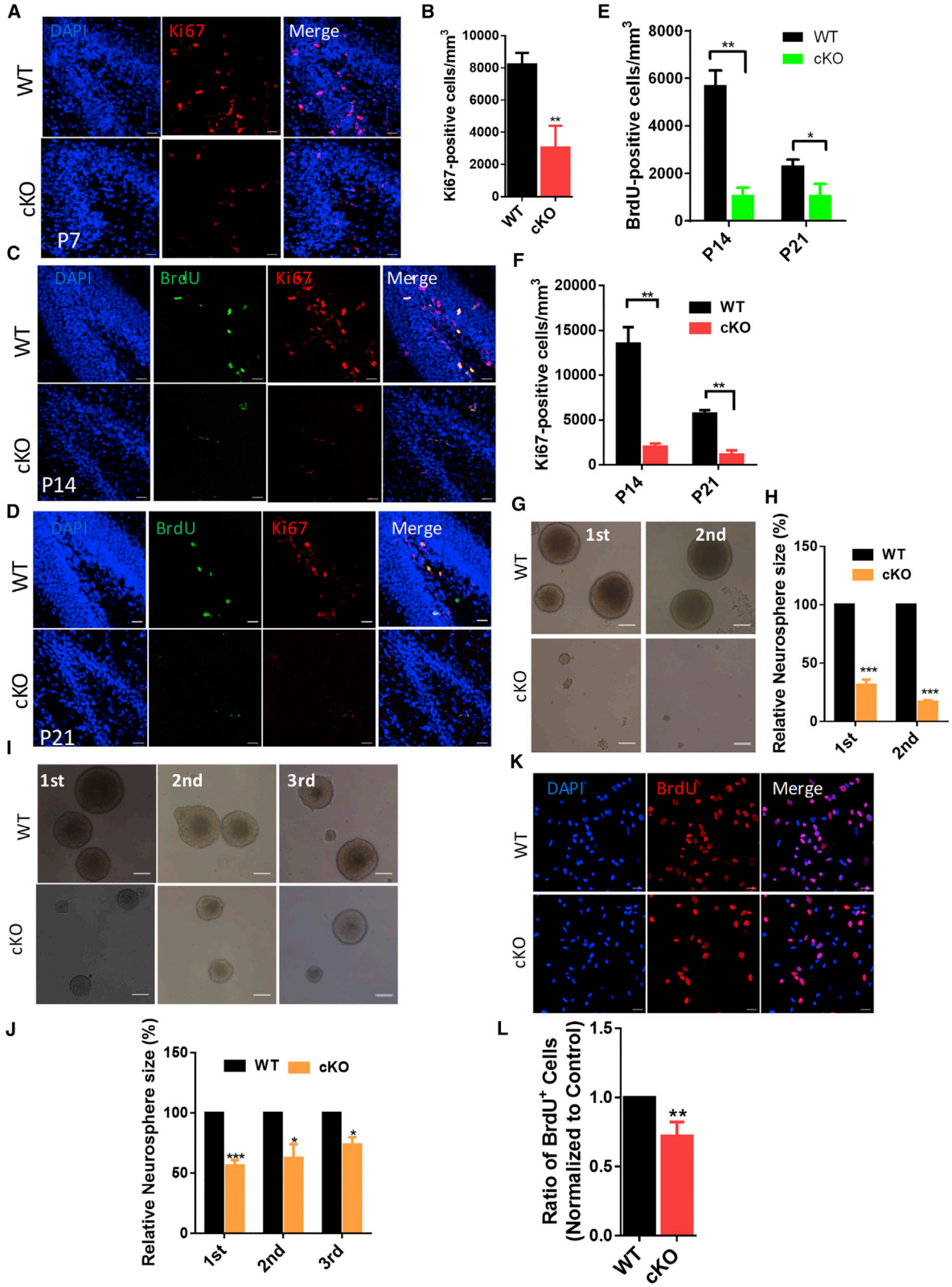

(legend on next page)

a significant reduction in self-renewing division. Meanwhile, EED-depleted NSPCs isolated from the forebrain formed smaller neurospheres than those from the WT, while there was no difference in the viability of NSPCs (Figures 5I and 5J). To further investigate the proliferation potential of NSPCs *in vitro*, we digested the primary neurospheres and plated 10,000 cells for BrdU incorporation and staining (after 6 h of labeling). We found that inactivation of EED reduced the proliferation ability of NSPCs *in vitro* (Figures 5K and 5L).

To determine whether elevated apoptosis is responsible for the loss of NSCs in postnatal EED cKO brains, we analyzed DG at P7 and observed apoptosis in these tissues, which is indicated by positive cells for terminal deoxynucleotidyl transferase dUTP nick-end labeling in the DG of hippocampus (Figures S4A and S4B). To further test if EED overexpression is sufficient to promote neurogenesis, we infected NSPCs isolated from WT mice with lentivirus expressing either GFP or human EED under the control of a CMV promoter. After 48 h, EED overexpression increased proliferation and differentiation in WT NSPCs (Figures S4C–S4F), demonstrating that EED is sufficient to promote NSPCs proliferation and differentiation. Together, these results suggest that EED is an important regulator of NSPC proliferation, and loss of EED impaired the amplification of NSPCs in DG.

EED Directly Targets the *Cdkn2a* Locus and Is Required for the Proliferation of DG NSPCs

The above-mentioned results suggest that EED is important for promoting neurogenesis and DG formation. Next, we aimed to unravel the molecular mechanisms mediated by EED in DG. To do so, we conducted a genome-wide analysis of mRNA levels (RNA sequencing [RNA-seq]) with two biological replicates from P14 DG. Following total RNA collection, we performed next-generation sequencing to identify differentially expressed genes (DEGs) between WT and EED cKO DG. EED deletion in DG caused dramatic change of genome-wide gene expression (Figures 6A, S5A, and S5B). A total of 561 upregulated and 486 downregulated genes were identified in EED cKO mice compared with WT mice (Figure 6A). To identify the biological functions perturbed by EED deletion, we subjected the DEGs to gene ontology analysis of biological processes. We found that genes downregulated on EED ablation are involved in forebrain development, neuronal differentiation, and cell growth, as well as other pathways that are critical for neurogenesis or DG formation (Figure 6B). Similarly, upregulated genes in EED cKO samples were enriched for processes related to regulation of cell fate and nervous system development (Figure 6B). From these analysis results, we speculate that EED regulates multiple cellular pathways to achieve its functions to maintain NSPCs at early stages and ensure proper neuronal differentiation and DG formation at later stages. To further identify candidate downregulated regulatory factors, we applied two bioinformatics tools, category net plot linkages of genes and biological concepts as a network and volcano plot. Interestingly, *Prox1* and *Sox11* are on the top of the list of genes that are correlated most significantly with neuronal property determination (Figures 6C and S5D). The Allen Brain Atlas shows that the mRNAs of *Prox1* and *Sox11* genes are enriched in the neurogenic regions of the mouse brain (date not shown). Thus, *Prox1* and *Sox11* genes could be candidate genes that are regulated by EED during neurogenesis. Consistently, enrichment analysis of upregulated genes after EED deletion also identified "p53 signaling

Figure 5. EED Ablation in DG NSPCs Impairs Their Proliferation Both *In Vivo* and *In Vitro*

(A) Immunostaining for Ki67 (red) in P7 DG of hippocampus from WT and EED cKO mice. Scale bars, 20 μm.

(B) Quantification of the percentage of $Ki67^+$ cells in the DG of WT and EED cKO at P7 mice (n = 3 mice). **p = 0.0084.

(C and D) Representative images of BrdU (green) and Ki67 (red) staining in the DG of hippocampus at P14 (C) and P21 (D). Scale bars, 20 μm.

(E) Quantification of $BrdU^+$ cells within the DG of WT and EED cKO mice at P14 and P21 (n = 3 mice for each). For P14, **p = 0.0027; for P21, *p = 0.0371.

(F) Quantification of $Ki67^+$ cells within the DG of WT and EED cKO mice at P14 and P21 (n = 3 mice for each). For P14, **p = 0.0035; for P21, **p = 0.0020.

(G) Primary (first) and secondary (second) neurospheres from WT and EED cKO mice at P0 DG. Representative P0 phase contrast images are shown. Scale bars, 100 μm.

(H) Quantification of size of primary and secondary neurospheres from three independent experiments are shown (n = 3). ***p = 0.0001.

(I and J) Representative images (I) and quantification (J) of primary (first), secondary (second), and tertiary (third) neurospheres from WT and EED cKO mice at P0 forebrain (n = 3 repeats at least). Scale bars, 100 μm. For first, ****p < 0.0001; for second, *p = 0.0394; for third, *p = 0.0137.

(K and L) Proliferation analyses showed that EED deletion reduced the proliferation of primary NSCs/progenitor cells. Cells were isolated from P0 DG and proliferation progenitor cells were labeled with BrdU (red) and then stained with BrdU antibody (K). (L) Quantitative comparison showed that the number of $BrdU^+$ progenitor cells in the EED deletion cells was smaller than in the control cells (n = 4). Scale bars, 20 μm. **p = 0.0015.

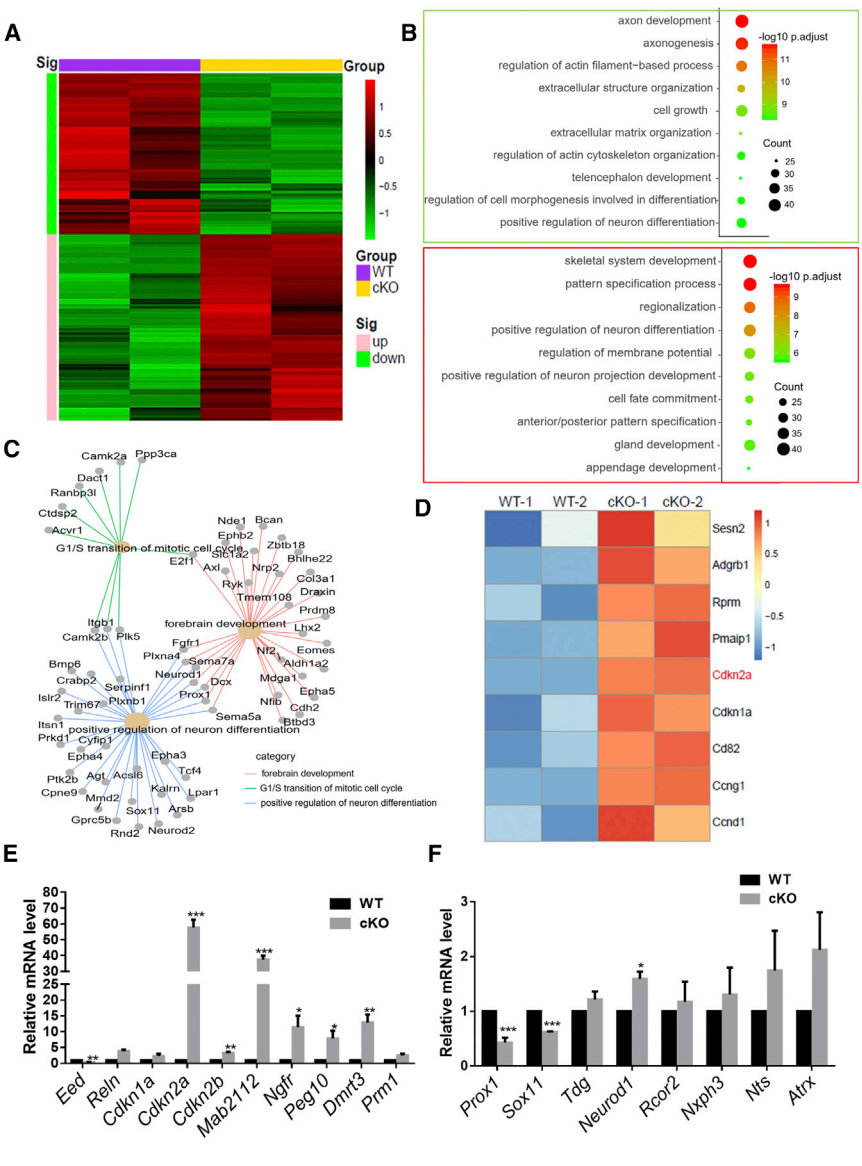

Figure 6. RNA-Seq and Functional Classification Reveals Diverse Genes Misregulated within the Dentate Gyrus of EED cKO Mice

(A) Heatmaps of 1,047 candidate genes that were differentially expressed with biological functional groups s compared between WT and EED cKO mice for P14 DG tissues. Expression is plotted as DESeq2 vsd-normalized RNA-seq counts with groups averaged and scaled by rows.

(B) Genes generated from RNA-seq analysis that were annotated using the functional annotation tool of GOEAST, revealing key biological processes that were downregulated (top) and upregulated (bottom) in the DG tissue of EED cKO mice.

(C) The category netplot depicted the linkages of downregulated genes and three biological concepts that are related to neuron development as a network.

(D) Heatmaps of upregulated genes that are related to cell proliferation. Expression is plotted as DESeq2 vsd-normalized RNA-seq counts with groups averaged and scaled by rows.

(E) Real-time qPCR analysis of RNA-seq-identified EED targets in the DG of WT and EED cKO mice at P14 (performed in triplicates). The level of GAPDH transcripts was used for normalization (n = 3 mice at least). *Cdkn1a*, p = 0.1664; *Prm1*, p = 2.631; *p < 0.05, **p < 0.01, ***p < 0.001.

(F) RNA expression of indicated genes in the DG of WT and EED cKO mice at P14 (performed in triplicates) were determined by qRT-PCR (n = 3 mice at least). *Tdg*, p = 0.2075; *Rcor2*, p = 0.6679; *Nxph3*, p = 0.5692; *Nts*, p = 0.3618; *Atrx*, p = 0.1784. *p < 0.05, ***p < 0.001.

pathway," which is related to cell proliferation (Figure S5C). *Cdkn2a* (also known as Ink4a/Arf) could be one candidate gene which might be related to cell proliferation (Figures 6D, S5C, and S5D). We then validated a subset of downregulated (*Sox11*, *Prox1*) and upregulated (*Cdkn2a*, *Mab21l2*, *Ngfr*, *Dmrt3*, and *Peg10*) genes related to the phenotypes observed in our study via real-time qPCR (Figures 6E and 6F). Our results confirmed that there is a marked increase in the expression of cyclin-dependent kinase inhibitors, including *Cdkn2a* and *Cdkn2b*, and a reduction in neuronal differentiation-promoting genes in EED cKO DG, such as *Prox1* and *Sox11*. Together, these analyses suggest that EED plays an essential role in regulating postnatal genes necessary for proper DG development.

In multiple adult stem cell populations, proliferation is regulated by PcG members via repression of CDKN2A, which encodes the $P16^{Ink4a}$ and $P19^{Arf}$ cell cyclin-dependent kinase inhibitors (Aoki et al., 2010; Ezhkova et al., 2009; Hwang et al., 2014; Molofsky et al., 2003; Xie et al., 2014). Our results showed that the *Cdkn2a* gene has the highest elevated expression level among all the tested genes after EED ablation (Figure 6E). In addition, using a $P19^{Arf}$-specific antibody, western blot analysis revealed an increased $P19^{Arf}$ protein level in EED cKO neurospheres cultured from the neonatal DG (Figures S6A and S6B), suggesting that *Cdkn2a* might be a direct downstream target of EED in DG NSPCs. EED, one of the PRC2 components, plays an essential role in the epigenetic maintenance of the H3K27me3 repressive chromatin mark. We then

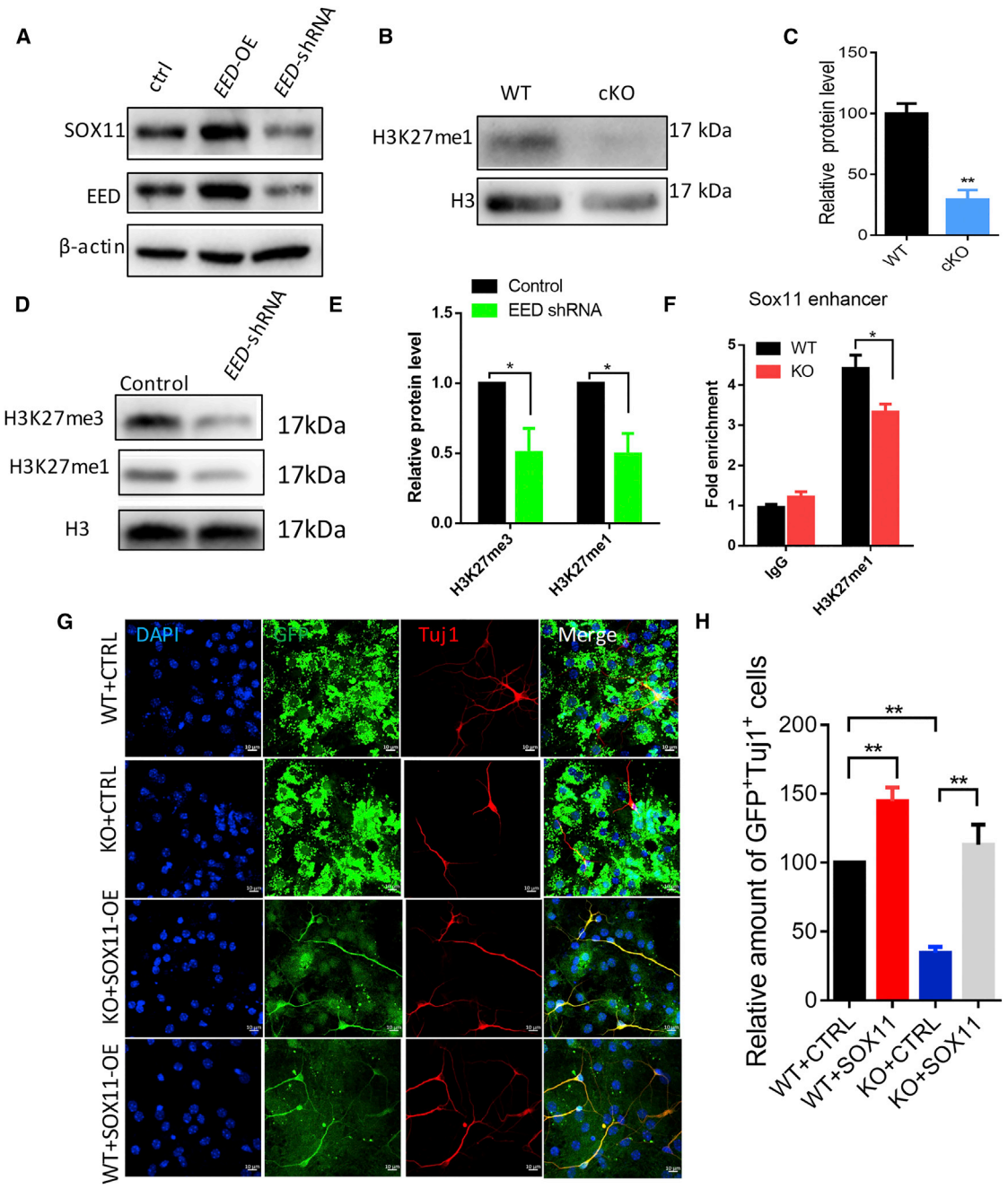

Figure 7. EED Regulates Neuronal Differentiation through Targeting *Sox11*

(A) Representative western blots shown for SOX11, EED, and β-actin (loading control, left panel). Knockdown of EED in cultured P0 neurosphere cells resulted in reduced expression of SOX11, and overexpression of EED in cultured P0 neurosphere cells resulted in enhanced expression of SOX11.

(B) Western blot analysis of the H3K27me1 methylation levels in cultured P0 neurosphere cells from WT and EED cKO mice. Histone H3 was used as the loading control.

(C) Quantification of the western blot in (B). The intensity of the H3K27me1 bands was normalized to that of respective H3 bands. For comparison, each dataset was normalized to the control (n = 3 mice). **p = 0.0034.

(D) Knockdown of EED in cultured mouse NSPCs western blots shown for H3K27me3, H3K27me1, and H3 (loading control).

(E) Quantification of protein expression levels in (D) normalized to H3 (n = 3 repeats at least). *p < 0.05.

(legend continued on next page)

explored whether EED directly regulates *Cdkn2a* in NSPCs by performing H3K27me3-specific chromatin immunoprecipitation (ChIP) in isolated P0 DG NSPCs from WT and EED cKO littermates, and analyzing the interaction between H3K27me3 and the genomic region of *Cdkn2a* gene through ChIP followed by qPCR. We found a stronger enrichment of H3K27me3 in the genomic region of *Cdkn2a* in EED WT NSPCs relative to that in EED cKO NSPCs (Figure S6C). Importantly, EED-specific ChIP further verified that EED is recruited to the *Cdkn2a* genomic locus (Figure S6C). These observations are consistent with a decrease in the global H3K27me3 level in the EED cKO versus WT mice (Figure 1I) and suggest that EED as part of the canonical PRC2 complex facilitates repression of its target gene *Cdkn2a*.

To further test whether *Cdkn2a* is a functional downstream target of EED and whether repression of *Cdkn2a* can rescue the proliferation defect in EED-deleted forebrain NSPCs, we used two distinct small hairpin RNAs (shRNAs) (CDKN2A-shRNA1 and CDKN2A-shRNA2) to downregulate CDKN2A expression in DG NSPCs. Transfection of NSPCs with these two shRNAs led to a robust reduction of endogenous *Cdkn2a* expression at both mRNA and protein levels (Figures S6D and S6E). We then explored whether CDKN2A deficiency could reverse the proliferation defect of EED ablation in NSPCs. NSPCs were isolated and infected with lentivirus expressing GFP alone or together with CDKN2A-shRNA for BrdU labeling. Upon knockdown of CDKN2A and deletion of EED, we did not observe a difference in the proportion of $BrdU^+$ cells in EED cKO NSPCs compared with WT NSPCs (Figures S6F and S6G). Together, these data suggest that *Cdkn2a* is critical for EED-mediated proliferation of DG NSPCs.

We next tested whether downregulation of CDKN2A could rescue the differentiation defect in EED-deleted NSPCs from DG. We infected EED cKO DG NSPCs with a lentivirus that expresses either CDKN2A-shRNA and GFP or a control GFP vector 1 day before the initiation of differentiation. CDKN2A-shRNA infected cells produced similar numbers of $Tuj1^+$ cells compared with the control group (Figures S6H and S6I). This result suggests that *Cdkn2a* may not be an essential functional downstream target of EED in regulating neuronal differentiation.

EED Modulates Neuronal Differentiation by Regulating Sox11 in DG

In support of our findings related to defects in DGC differentiation in EED-ablated mice, we noticed that *Sox11* and *Prox1*, two important transcription factors involved in neurogenesis, were significantly downregulated within the DG of EED cKO mice (Figure 6F). We reason that EED might directly promote neurogenesis via regulation of differentiation-related transcription factors, such as *Sox11* and *Prox1*. To test this idea, we first expressed exogenous EED by lentivirus infection and assayed the expression of SOX11 protein by western blot. As expected, overexpression of EED can promote SOX11 protein level in cultured NSPCs from the neonatal DG (Figure 7A). Importantly, immunostaining results showed that the expression of SOX11 is reduced in SGZ of EED cKO mice (Figure S7A). Furthermore, we selectively ablated EED in granular neurons using $Eed^{f/f}$;Nex-Cre^+ (expresses Cre recombinase at E11.5) mice. In $Eed^{f/f}$;Nex-Cre^+ (cKO) mice, SOX11 expression was indeed reduced in the DG neurons of EED mutants (Figures S7B and S7C). We then performed ChIP assays to examine whether loss of EED leads to changes of H3K27 methylation on the promoters of the *Sox11* and *Prox1* genes. ChIP-qPCR analysis showed no changes of H3K27me3 on the promoters of *Sox11* and *Prox1* genes in EED mutant NSPCs (Figure S7D). Several reports have shown that histone 3 lysine 27 mono-methylation (H3K27me1) accumulates within transcribed genes and promotes transcription (Cui et al., 2009; Ferrari et al., 2014; Steiner et al., 2011). The downregulation of SOX11 and PROX1 in EED cKO mice led us to hypothesize that H3K27me1 might accumulate at *Sox11* and *Prox1* promoters and then activate *Sox11* and *Prox1* transcription. To directly test this notion, we first measured the global H3K27me1 level in EED cKO NSPCs from DG. As expected, western blot analysis showed a significant reduction of H3K27me1 level in NSPCs isolated from EED cKO mice (Figures 7B and 7C). In addition, infection of cultured mouse NSPCs with EED shRNA also caused a significant reduction in H3K27me3 and H3K27me1 (Figures 7D and 7E). Consistent with the downregulation of *Sox11* gene expression, ChIP-qPCR analysis revealed that there was no significant enrichment of H3K27me1 at the *Prox1* promoter (Figure S7E), but a decrease of H3K27me1 enrichment at the promoter or enhancer of *Sox11* gene in EED cKO NSPCs relative to that in WT NSPCs (Figures 7F

(F) ChIP-qPCR analysis. ChIP was performed using anti-IgG, anti-H3K27me1 antibodies, and PCR analysis was performed with the primers indicated. Each bars are represented as fold enrichment of immunoprecipitated DNA from each sample relative to the DNA immunoprecipitated with the IgG antibody (control). *p = 0.0474.

(G) Infection of P0 neural stem cells with control, SOX11-OE virus co-expressing GFP under the CMV promoter (green). The differentiation ability of P0 neural stem cells was assessed by $Tuj1^+$ cells (red). DAPI, blue.

(H) Quantification of $Tuj1^+$ GFP^+ cells as a fraction of all GFP^+ cells in EED cKO NSPCs that were infected with SOX11-OE virus compared with those in EED cKO NSPCs that were infected with control virus (n = 3 repeats at least). Scale bars, 20 μm. **p < 0.01.

and S7F). Together, these results suggest that EED might activate *Sox11* expression by mediating H3K27me1at the *Sox11* promoter or enhancer and maintaining an open chromatin structure.

Finally, to test whether increased SOX11 levels in EED-deleted NSPCs could rescue their neuronal differentiation defect, we overexpressed SOX11 in cultured P0 NSPCs. Real-time PCR and western blot analysis confirmed that the expression of *Sox11* was significantly higher in the SOX11 overexpression group compared with the control (Figures S7G and S7H). EED cKO NSPCs with SOX11-overexpression produced more Tuj1$^+$ cells after 10 days of differentiation compared with cells infected with the control lentivirus (Figures 7G and 7H), indicating that overexpression of SOX11 could restore the neuronal differentiation defect caused by EED deletion. Taken together, these results suggest that *Sox11* is a functional downstream target of EED in modulating neuronal differentiation.

DISCUSSION

One of the fundamental questions in brain development is how NSPCs give rise to various neuronal and glial cell types in a defined order to achieve appropriate organization. The DG is the primary input to the hippocampus and plays important roles in learning, memory, and adult neurogenesis (Hevner, 2016). In this study, by generating a cKO mouse model, we provide direct evidence showing that the PcG protein EED is required for the proper formation of DG neurogenesis. Molecularly, we have identified *Ink4a/Arf (Cdkn2a)* and *Sox11* as key downstream targets of EED in the DG carrying out distinct and separate functions in modulating proliferation and differentiation of NSPCs. Although our results suggest that EED may play different roles in the differentiation of different cell subtypes, we cannot ascertain a cell-autonomous function of EED for each cell type in the DG. Further studies are needed to further clarify how EED regulates the generation and maturation of various cell types within DG.

EED has a Crucial Role in Postnatal Reorganization of Dentate Precursor and Granule Cells

Several lines of evidence have shown that PRC2 components are highly expressed in both embryonic and adult NSPCs. Thus, it is not surprising that PRC2 has multiple functions during neurogenesis at distinct stages, such as self-renewal of NSPCs, neuronal-glial fate specification, and maturation (Guillemot, 2007). Our group recently found that the EZH2-miR-203-BMI1 signaling axis is critical for regulating the proliferation of both embryonic and adult NSPCs (Liu et al., 2017). Here, we extend our previous study by developing a cKO mouse model and investigating the brain-specific role of EED, another PRC2 component during prenatal and postnatal development. To this end, we have for the first time provided functional and molecular evidence supporting an essential role of EED and EED-mediated H3K27 methylation in the reorganization of dentate precursors and DG development.

At birth, the hilus of the DG is filled with mixed precursors and newborn neurons. During the first postnatal week, this rather amorphous mass undergoes a conversion into a highly radially organized structure. This reorganization is apparently important for the continuous generation and proper distribution of granule cells (Tian et al., 2012). Our results suggest that EED-driven H3K27methylation may have a significant involvement in this reorganization process. Deletion of EED severely impaired the formation of the SGZ. GFAP$^+$ cells were significantly reduced and dentate progenitors and granule cells were aberrantly distributed in the EED cKO hippocampus. In EED cKO mice, the volumes of both the upper and lower blades of DG were reduced compared with the WT group. Molecularly, our RNA-seq profiling data identified a number of genes related to anterior/posterior pattern specification that were differentially expressed in EED cKO DG, suggesting an important role of EED in the anterior/posterior pattern specification. Consistent with this notion, EED has been previously demonstrated as a global regulator of anterior-posterior patterning in mice (Faust et al., 1998; Schumacher et al., 1996). Furthermore, mice homozygous for a null allele of *Eed* displayed a growth defect and failed to gastrulate normally (Schumacher et al., 1996). Therefore, our findings have not only confirmed a critical role of EED for pattern organization but also provided molecular insight into the mechanisms underlying this elegant process.

EED Modulates Self-Renewal and Differentiation of NSPCs in the DG

Earlier reports have demonstrated that EED-null mice exhibit a growth defect and fail to gastrulate normally (Schumacher et al., 1996). The lack of neural induction in these animals suggests an essential role of EED in neuroectodermal development. In this study, our newly developed brain-specific knockout mouse model has allowed, for the first time, an assessment of the neurogenic function of EED during prenatal and postnatal development. Brain-specific depletion of EED dramatically decreased the proliferation of NSPCs and impaired neuronal differentiation and oligodendrocyte differentiation during DG development. These neurogenic defects in DG represent the most striking phenotype in these animals, thus directly reflecting a major function of EED during hippocampal neurogenesis. Furthermore, the essential role of EED in hippocampal neurogenesis is expected to have a significant

impact on learning and memory, as mammalian information storage relies on the generation and incorporation of newborn neurons in the hippocampus (Deng et al., 2010). Importantly, clinical evidence has demonstrated that an EED mutation can cause Weaver syndrome, an autosomal dominant disease characterized by learning disabilities. Further behavioral tests on our EED cKO mice will likely shed light on the cognitive functions of EED in regulating hippocampus-dependent learning and memory.

Distinct and Separable Roles for EED in Regulating Proliferation and Differentiation of NSPCs

In addition to tri-methylated state, H3K27 is also modified in mono- and di-methylated states. PRC2 activity is not only associated with H3K27me3 but also modulates all forms of H3K27 methylation in a spatially defined manner, contributing to different genomic functions in mouse embryonic stem cells (Ferrari et al., 2014). Previous evidence suggests that EED is responsible for catalyzing mono-, di-, and tri-methylation of histone H3 at lysine 27 (H3K27me1/2/3) (Ferrari et al., 2014) and regulates development by modulating gene transcription. In line with the theory that PRC2-dependent H3K27me1 deposition positively correlates with active transcription, we found that ablation of EED in DG significantly reduced the expression level of SOX11, an important regulator for adult neurogenesis (Feng et al., 2013).

The transition from NSPCs proliferation to differentiation depends on different gene expression states. We have identified and characterized EED as a key mediator of the transition from NSPCs proliferation to neural differentiation. Our study clearly suggested that highly expression of EED is required for proper NSPCs proliferation that depends on *Cdkn2a*. When EED is deleted, critical genes (i.e., *Sox11*) for neural differentiation are repressed, indicating that EED appears to mainly act as an activator for modulating the expression of genes responsible for proliferation and differentiation. The precise mechanisms underlying EED-mediated gene activation remain largely unknown. Further studies will reveal the upstream regulators of EED and how the gene-regulatory network perturbation shifts proliferation to differentiation of NSPCs.

Taken together, our study established EED as an important modulator of NSPCs in neurogenesis and DG formation in the mouse brain. Furthermore, we identified distinct and separable roles of EED in the production of new neurons from NSPCs. These results provide novel mechanistic insights into the complex role that EED plays in brain development. Emerging evidence suggests that abnormal PRC2 expression may cause neurological diseases. For example, mutations in EZH2 or EED are associated with Weaver syndrome (Cooney et al., 2017; Imagawa et al., 2017), and account for intellectual disability in patients (Tatton-Brown et al., 2017). Given the essential role of DG development in the pathogenesis of neurological disorders, our data thus not only establish a critical role of EED in mouse hippocampal neurogenesis and development, but also shed new light on the molecular underpinnings of EED mutations that lead to intellectual disability in human neurological disorders, including Weaver's syndrome.

EXPERIMENTAL PROCEDURES

Detailed descriptions of experimental procedures can be found in the Supplemental Information.

Animals

All mice used in the current study have a C57BL6 background. All mouse experiments were approved by the Animal Committee of the Institute of Zoology, Chinese Academy of Sciences, Beijing, China (for details, see Supplemental Experimental Procedures).

Cell Culture

Primary NSPCs were isolated (Liu et al., 2017) as described in detail in the Supplemental Experimental Procedures.

H&E and Immunostaining

Immunofluorescence was performed as described previously (Liu et al., 2017). For more details, please see the Supplemental Experimental Procedures.

Western Blot

Samples were prepared and analyzed as described in detail in the Supplemental Experimental Procedures.

ACCESSION NUMBERS

The original RNA-seq data from this study are available at the NCBI Gene Expression Omnibus (http://www.ncbi.nlm.nih.gov/geo/) under accession number GEO: GSE131035.

SUPPLEMENTAL INFORMATION

Supplemental Information can be found online at https://doi.org/10.1016/j.stemcr.2019.05.010.

AUTHOR CONTRIBUTIONS

Z.-Q.T. and C.-M.L., conception and design, collection and assembly of data, data analysis and interpretation, manuscript writing, and final approval of manuscript. P.-P.L., Y.-J.X., S.-K.D., H.-Z.D., Y.-Y.W., and X.-G.L., collection and assembly of data.

ACKNOWLEDGMENTS

The authors gratefully acknowledge Dr. Stuart H. Orkin at Harvard Medical School for providing $Eed^{f/f}$ mice, Dr. Shyh-Chang Ng for editing the manuscript. This work was supported by grants from

the Strategic Priority Research Program of the Chinese Academy of Sciences (grant no. XDA16010302 and XDA16010304), the National Key Research and Development Program of China Project (2016YFA0101402), and the National Science Foundation of China (91753140). The authors declare no competing financial interests.

Received: November 21, 2018
Revised: May 12, 2019
Accepted: May 13, 2019
Published: June 13, 2019

REFERENCES

Aoki, R., Chiba, T., Miyagi, S., Negishi, M., Konuma, T., Taniguchi, H., Ogawa, M., Yokosuka, O., and Iwama, A. (2010). The polycomb group gene product Ezh2 regulates proliferation and differentiation of murine hepatic stem/progenitor cells. J. Hepatol. *52*, 854–863.

Cooney, E., Bi, W., Schlesinger, A.E., Vinson, S., and Potocki, L. (2017). Novel EED mutation in patient with Weaver syndrome. Am. J. Med. Genet. A *173*, 541–545.

Cui, K., Zang, C., Roh, T.Y., Schones, D.E., Childs, R.W., Peng, W., and Zhao, K. (2009). Chromatin signatures in multipotent human hematopoietic stem cells indicate the fate of bivalent genes during differentiation. Cell Stem Cell *4*, 80–93.

Deng, W., Aimone, J.B., and Gage, F.H. (2010). New neurons and new memories: how does adult hippocampal neurogenesis affect learning and memory? Nat. Rev. Neurosci. *11*, 339–350.

Ezhkova, E., Pasolli, H.A., Parker, J.S., Stokes, N., Su, I.H., Hannon, G., Tarakhovsky, A., and Fuchs, E. (2009). Ezh2 orchestrates gene expression for the stepwise differentiation of tissue-specific stem cells. Cell *136*, 1122–1135.

Faust, C., Lawson, K.A., Schork, N.J., Thiel, B., and Magnuson, T. (1998). The Polycomb-group gene eed is required for normal morphogenetic movements during gastrulation in the mouse embryo. Development *125*, 4495–4506.

Feng, W.J., Khan, M.A., Bellvis, P., Zhu, Z., Bernhardt, O., Herold-Mende, C., and Liu, H.K. (2013). The chromatin remodeler CHD7 regulates adult neurogenesis via activation of SoxC transcription factors. Cell Stem Cell *13*, 62–72.

Ferrari, K.J., Scelfo, A., Jammula, S., Cuomo, A., Barozzi, I., Stutzer, A., Fischle, W., Bonaldi, T., and Pasini, D. (2014). Polycomb-dependent H3K27me1 and H3K27me2 regulate active transcription and enhancer fidelity. Mol. Cell *53*, 49–62.

Freund, T.F., and Buzsaki, G. (1996). Interneurons of the hippocampus. Hippocampus *6*, 347–470.

Guillemot, F. (2007). Spatial and temporal specification of neural fates by transcription factor codes. Development *134*, 3771–3780.

Han, Y.G., Spassky, N., Romaguera-Ros, M., Garcia-Verdugo, J.M., Aguilar, A., Schneider-Maunoury, S., and Alvarez-Buylla, A. (2008). Hedgehog signaling and primary cilia are required for the formation of adult neural stem cells. Nat. Neurosci. *11*, 277–284.

Hevner, R.F. (2016). Evolution of the mammalian dentate gyrus. J. Comp. Neurol. *524*, 578–594.

Hirabayashi, Y., Suzki, N., Tsuboi, M., Endo, T.A., Toyoda, T., Shinga, J., Koseki, H., Vidal, M., and Gotoh, Y. (2009). Polycomb limits the neurogenic competence of neural precursor cells to promote astrogenic fate transition. Neuron *63*, 600–613.

Hwang, W.W., Salinas, R.D., Siu, J.J., Kelley, K.W., Delgado, R.N., Paredes, M.F., Alvarez-Buylla, A., Oldham, M.C., and Lim, D.A. (2014). Distinct and separable roles for EZH2 in neurogenic astroglia. Elife *3*, e02439.

Imagawa, E., Higashimoto, K., Sakai, Y., Numakura, C., Okamoto, N., Matsunaga, S., Ryo, A., Sato, Y., Sanefuji, M., Ihara, K., et al. (2017). Mutations in genes encoding polycomb repressive complex 2 subunits cause Weaver syndrome. Hum. Mutat. *38*, 637–648.

Liu, P.P., Tang, G.B., Xu, Y.J., Zeng, Y.Q., Zhang, S.F., Du, H.Z., Teng, Z.Q., and Liu, C.M. (2017). MiR-203 interplays with polycomb repressive complexes to regulate the proliferation of neural stem/progenitor cells. Stem Cell Reports *9*, 190–202.

Margueron, R., Justin, N., Ohno, K., Sharpe, M.L., Son, J., Drury, W.J., Voigt, P., Martin, S.R., Taylor, W.R., De Marco, V., et al. (2009). Role of the polycomb protein EED in the propagation of repressive histone marks. Nature *461*, 762–U711.

Molofsky, A.V., Pardal, R., Iwashita, T., Park, I.K., Clarke, M.F., and Morrison, S.J. (2003). Bmi-1 dependence distinguishes neural stem cell self-renewal from progenitor proliferation. Nature *425*, 962–967.

Pereira, J.D., Sansom, S.N., Smith, J., Dobenecker, M.W., Tarakhovsky, A., and Livesey, F.J. (2010). Ezh2, the histone methyltransferase of PRC2, regulates the balance between self-renewal and differentiation in the cerebral cortex. Proc. Natl. Acad. Sci. U S A *107*, 15957–15962.

Satijn, D.P., Hamer, K.M., den Blaauwen, J., and Otte, A.P. (2001). The polycomb group protein EED interacts with YY1, and both proteins induce neural tissue in *Xenopus* embryos. Mol. Cell. Biol. *21*, 1360–1369.

Schumacher, A., Faust, C., and Magnuson, T. (1996). Positional cloning of a global regulator of anterior-posterior patterning in mice. Nature *384*, 648.

Shen, X., Liu, Y., Hsu, Y.J., Fujiwara, Y., Kim, J., Mao, X., Yuan, G.C., and Orkin, S.H. (2008). EZH1 mediates methylation on histone H3 lysine 27 and complements EZH2 in maintaining stem cell identity and executing pluripotency. Mol. Cell *32*, 491–502.

Steiner, B., Kronenberg, G., Jessberger, S., Brandt, M.D., Reuter, K., and Kempermann, G. (2004). Differential regulation of gliogenesis in the context of adult hippocampal neurogenesis in mice. Glia *46*, 41–52.

Steiner, L.A., Schulz, V.P., Maksimova, Y., Wong, C., and Gallagher, P.G. (2011). Patterns of histone H3 lysine 27 monomethylation and erythroid cell type-specific gene expression. J. Biol. Chem. *286*, 39457–39465.

Tatton-Brown, K., Loveday, C., Yost, S., Clarke, M., Ramsay, E., Zachariou, A., Elliott, A., Wylie, H., Ardissone, A., Rittinger, O., et al. (2017). Mutations in epigenetic regulation genes are a major cause

of overgrowth with intellectual disability. Am. J. Hum. Genet. *100*, 725–736.

Tian, C.X., Gong, Y.F., Yang, Y., Shen, W., Wang, K., Liu, J.H., Xu, B.K., Zhao, J., and Zhao, C.J. (2012). Foxg1 has an essential role in postnatal development of the dentate gyrus. J. Neurosci. *32*, 2931–2949.

von Schimmelmann, M., Feinberg, P.A., Sullivan, J.M., Ku, S.M., Badimon, A., Duff, M.K., Wang, Z., Lachmann, A., Dewell, S., Ma'ayan, A., et al. (2016). Polycomb repressive complex 2 (PRC2) silences genes responsible for neurodegeneration. Nat. Neurosci. *19*, 1321–1330.

Xie, H., Xu, J., Hsu, J.H., Nguyen, M., Fujiwara, Y., Peng, C., and Orkin, S.H. (2014). Polycomb repressive complex 2 regulates normal hematopoietic stem cell function in a developmental-stage-specific manner. Cell Stem Cell *14*, 68–80.

Zhang, J., Ji, F., Liu, Y., Lei, X., Li, H., Ji, G., Yuan, Z., and Jiao, J. (2014). Ezh2 regulates adult hippocampal neurogenesis and memory. J. Neurosci. *34*, 5184–5199.

Zhuo, L., Theis, M., Alvarez-Maya, I., Brenner, M., Willecke, K., and Messing, A. (2001). hGFAP-cre transgenic mice for manipulation of glial and neuronal function in vivo. Genesis *31*, 85–94.